GEM NEWS INTERNATIONAL

Contributing Editors
Gagan Choudhary, *IIGJ-Research & Laboratories Centre, Jaipur, India* (gagan.choudhary@iigjrlc.org)
Christopher M. Breeding, *GIA, Carlsbad* (christopher.breeding@gia.edu)
Guanghai Shi, *School of Gemmology, China University of Geosciences, Beijing* (shigh@cugb.edu.cn)

COLORED STONES AND ORGANIC MATERIALS

Blue amblygonite-montebrasite from Rwanda. Amblygonite-montebrasite, with the formula $LiAlPO_4(F,OH)$, is a fluorophosphate mineral series found in granitic pegmatites and pegmatite-related environments. The Pala district in California and the Black Hills in South Dakota are historic U.S. sources of amblygonite-montebrasite for industrial use, but most of the world's well-known pegmatite districts have also produced considerable quantities of amblygonite-montebrasite.

A relatively common rock-forming mineral in these specific environments, the mineral is typically opaque and contains abundant fractures. Its color is often an unremarkable creamy white, causing it to blend in with associated feldspars. All of these factors limit its use as a gemstone. When used as a gem material, it is often colorless to yellow-green.

Figure 1. The newly discovered variety of amblygonite-montebrasite is unique for its blue color. It often has a mottled appearance with alternating blue and creamy white patches. The faceted stone weighs 0.83 ct. Photo by Lhapsin Nillapat.

Geologists are interested in this mineral because of its high lithium content (up to 10%), which often suggests the presence of other (and easier to process) lithium minerals nearby. With increasing demand for lithium ores, exploration teams around the world are paying closer attention to amblygonite-montebrasite as an indicator of high lithium content in geological environments. This was the case in western Rwanda, an area known for its pegmatite-related tin deposits, where local geologists discovered an unusual variety of amblygonite-montebrasite in multiple pegmatites and sent it to mineral traders in Bangkok.

The new material (figure 1) differs from classic varieties in that its color is bright blue, sometimes associated with creamy white patches in a mottled pattern. All other characteristics match the known properties of amblygonite-montebrasite.

Confocal Raman spectroscopy showed a perfect match with amblygonite for several of the whitish and all of the bright blue patches. The position of certain peaks is related to the fluorine concentration in the mineral and can help to estimate the distribution between both end members (B. Rondeau et al., "A Raman investigation of the amblygonite-montebrasite series," *Canadian Mineralogist*, Vol. 44, No. 5, 2006, pp. 1109–1117). The position of the peak around 1060 cm^{-1} was in the lower range (1052 cm^{-1} or lower), which points to a very fluorine-poor composition, near pure montebrasite. Raman spectroscopy performed at

Editors' note: Interested contributors should send information and illustrations to Stuart Overlin at soverlin@gia.edu.

Gems & Gemology, Vol. 59, No. 4, pp. 524–542.

GIA's Bangkok laboratory also revealed the presence of other minerals in the creamy white matrix. This included a mix of complex phosphates that share mineralogical and chemical similarities (e.g., berlinite, souzalite, and trolleite, confirmed by Raman spectroscopy) as well as feldspar. The only exception in terms of coloration consisted of small dark blue spots of the mineral scorzalite, with the formula $(Fe^{2+},Mg)Al_2(OH,PO_4)_2$, a common secondary phase in complex, phosphate-rich pegmatites.

Despite advanced techniques indicating that this newly discovered variety, as well as the majority of previously documented gems, are closer to montebrasite (the OH-rich end member), the gemological community keeps referring to these materials as amblygonite. Amblygonite-montebrasite remains a rare gem that is unfamiliar to the general consumer. It requires considerable care due to its perfect cleavage and hardness of approximately 6, making it less suitable for daily wear. With this new addition to its color range, amblygonite-montebrasite might gain more recognition.

Wim Vertriest
GIA, Bangkok

Gil Yuda
Gil Yuda Mogok Minerals Ltd.
Bangkok

Joe Henley
Joe Henley Rough & Gemstones, LLC
Portland, Oregon

FTIR identification of carbon dioxide fluids in sapphire. Carbon dioxide is well known as a trapped fluid in negative crystals in sapphire. From room temperature to cooler temperatures, the negative crystals change from a single supercritical fluid phase to two phases of gas and liquid. This feature is fascinating to observe under the microscope (e.g., Spring 2016 *G&G* Micro-World, pp. 78–79). These fluid inclusions are considered proof that a sapphire has not undergone thermal treatment (e.g., J.I. Koivula, "Carbon dioxide fluid inclusions as proof of natural-colored corundum," Fall 1986 *G&G*, pp. 152–155).

However, the Summer 2020 issue of *G&G* reported on a sapphire heated with pressure that contained a carbon dioxide gas bubble even after treatment (N. Ng-Pooresatien, "Lab Notes: Negative crystal containing a mobile CO_2 bubble in blue sapphire heated with pressure," pp. 287–288). Most previous reports about carbon dioxide fluid inclusions were based on microscopic observation, but this one addressed the presence of carbon dioxide fluid using Fourier-transform infrared (FTIR) spectroscopy.

Figure 2 shows two sapphires from Sri Lanka and Myanmar with fluid inclusions of primary and secondary negative crystals. FTIR spectra of these two sapphires are presented in figure 3. The two peaks at 3601 and 3705 cm^{-1} are easily confused with kaolinite-related peaks at 3619 and 3698 cm^{-1}. All of the spectra show several peaks assigned to dense carbon dioxide vibration and combination overtone bands. The 2342 cm^{-1} peak is C=O asymmet-

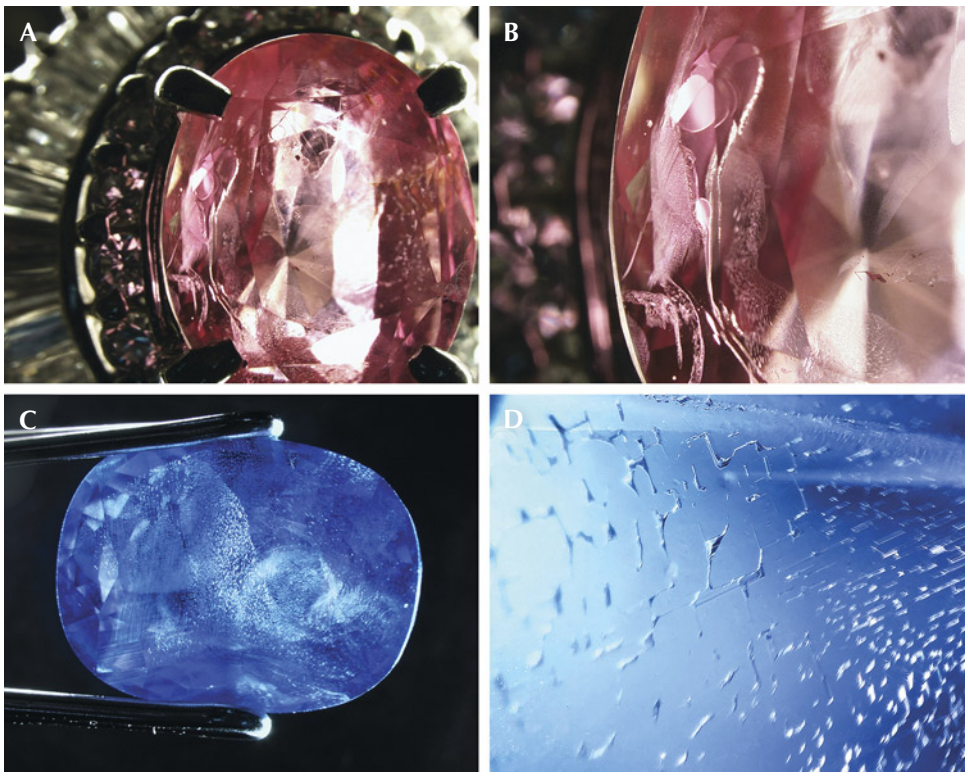

Figure 2. Various negative crystals in pink sapphire from Sri Lanka (A, enlarged in B) and fingerprints in blue sapphire from Myanmar (C, enlarged in D). Image B shows bubbles in flat negative crystals, and the center negative crystal in D has a bubble. Photomicrographs by Momo Matsumura (A and B) and Shunsuke Nagai (C and D); fields of view 4.05 mm (A), 8.15 mm (B), 8.47 mm (C), and 1.71 mm (D).

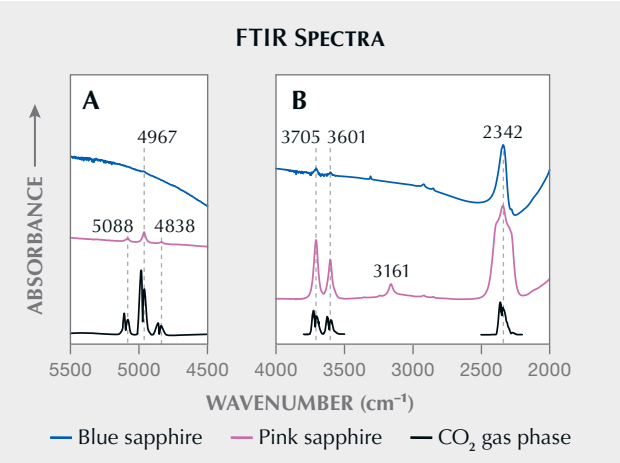

Figure 3. FTIR spectra of the two sapphires from figure 2 indicate dense carbon dioxide–assigned peaks from 2000 to 4000 cm^{-1} and 4500 to 5500 cm^{-1}. The two peaks at 3601 and 3705 cm^{-1} are easily mistaken for kaolinite peaks at 3619 and 3698 cm^{-1}.

ric stretching vibration ν_3. The 3601 and 3705 cm^{-1} peaks are $2\nu_2 + \nu_3$ and $\nu_1 + \nu_3$ first Fermi resonance, respectively. The 4838, 4967, and 5088 cm^{-1} peaks are $4\nu_2 + \nu_3$, $\nu_1 + 2\nu_2 + \nu_3$, and $2\nu_1 + \nu_3$ second Fermi resonance peaks, respectively, where ν_1 is a symmetric stretching and ν_2 is a doubly degenerate bending (table 1). Those peaks generally present double absorption bands, P- and R-contour, under atmospheric pressure and temperature due to the rotational transitions that occur for the stretching band, as seen in the bottom spectrum of figure 3. The double peaks change to a single peak, increasing the carbon dioxide fluid density by more than ~0.4 g/cm^3 (M. Buback et al., "Near infrared absorption of pure carbon dioxide up to 3100 bar and 500 K. I. Wavenumber range 3200 cm^{-1} to 5600 cm^{-1}," *Zeitschrift für Naturforschung A*, Vol. 41, 1986, pp. 505–511; A. Oancea et al., "Laboratory infrared reflection spectrum of carbon dioxide clathrate hydrates for astrophysical remote sensing applications," *Icarus*, Vol. 221, No. 2, 2012, pp. 900–910).

In order to prove the high density of carbon dioxide fluids, this author used micro-Raman spectroscopy. Raman spectra of carbon dioxide in fluid inclusions show a Fermi diad (or doublet) (figure 4), which is useful in estimating carbon dioxide fluid pressure and density in negative crystals (e.g., J. Yamamoto et al., "Paleo-Moho depth determined from the pressure of CO_2 fluid inclusions: Raman spectroscopic barometry of mantle- and crust-derived rocks," *Earth and Planetary Science Letters*, Vol. 253, 2007, pp. 369–377; H.M. Lamadrid et al., "Reassessment of the Raman CO_2 densimeter," *Chemical Geology*, Vol. 450, 2016, pp. 201–222). Using the equations reported by Lamadrid et al. (2016), carbon dioxide fluid densities in sapphires measured by FTIR spectra were estimated at 0.54–0.74 g/cm^3. This density is consistent with the results derived from FTIR spectra in figure 3.

TABLE 1. Carbon dioxide vibration band position (Buback et al., 1986; Oancea et al., 2012).[a]

Wavenumber (cm^{-1})	Mode/assignment
2342	C=O asymmetric stretching vibration ν_3
3601	$2\nu_2 + \nu_3$ (first Fermi resonance)
3705	$\nu_1 + \nu_3$ (first Fermi resonance)
4838	$4\nu_2 + \nu_3$ (second Fermi resonance)
4967	$\nu_1 + 2\nu_2 + \nu_3$ (second Fermi resonance)
5088	$2\nu_1 + \nu_3$ (second Fermi resonance)

[a] *ν_1 is a symmetric stretching, and ν_2 is a doubly degenerate bending.*

According to the Summer 2020 Lab Notes entry, sapphire with heat and pressure showed a strong broad peak at 3047 cm^{-1} with C=O asymmetric stretching vibration ν_3 at 2342 cm^{-1} and no other peaks at wavenumbers higher than 3600 cm^{-1}. The Raman spectra also revealed a carbon dioxide Fermi diad (N. Ng-Pooresatien, pers. comm., 2023), and the density was estimated to be 0.11–0.18 g/cm^3, which is about one-fifth lower. The existence of carbon dioxide bubbles in a negative crystal is therefore no longer definitive proof of the absence of thermal

Figure 4. Raman spectrum of carbon dioxide showing the Fermi diad (or doublet) from a negative crystal inclusion in a sapphire.

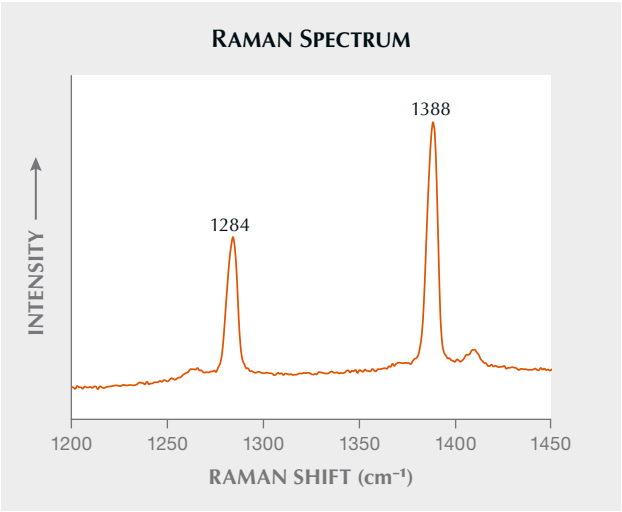

Figure 5. Demantoid garnet (0.84 ct on the left and 0.28 ct on the right) and an orange grossular garnet (0.55 ct) from Sonora, Mexico. Photo by Diego Sanchez.

treatment. This investigation also showed that FTIR analysis is a useful method for detecting the high density of carbon dioxide fluid in sapphire, and the resulting FTIR peaks above 3600 cm^{-1} could indicate the absence of heat treatment.

Kazuko Saruwatari
GIA, Tokyo

Demantoid, andradite, and grossular from Mexico. Iridescent andradite garnet is an interesting phenomenal stone that was initially produced in Nevada but has also been found in Mexico, Japan, and New Mexico. A small parcel consisting of three stones (figure 5) was recently submitted to GIA's Carlsbad laboratory and contained some new gem material from the iridescent andradite deposit in Mexico. The deposit is located high in the Sonoran Sierra in the Mexican state of Sonora about 145 km northeast of the city of Hermosillo. The stones were provided by Marion Alberto Márquez Suárez, who works with the mine owner, Salvador Barba.

Figure 6. Mineral inclusions in a Mexican demantoid. Photomicrograph by Aaron Palke; field of view 1.26 mm.

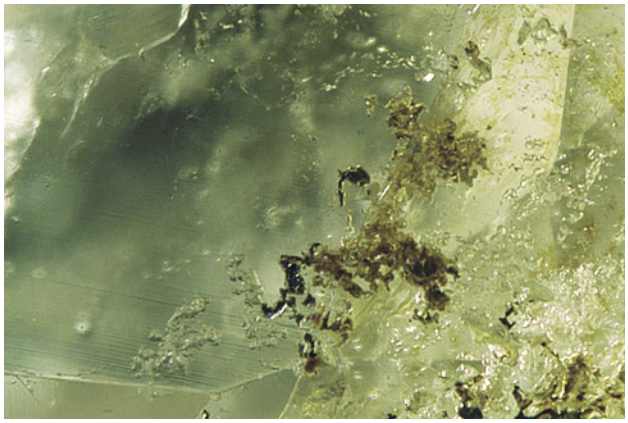

Standard gemological testing gave a refractive index of 1.740 for the grossular garnet and over-the-limit readings for the demantoid garnets. All three samples were inert to both long-wave and short-wave ultraviolet light. Fingerprints and fields of fluid inclusions as well as colorless and dark crystal inclusions were observed (figure 6). The inclusion scenes were reminiscent of skarn-related demantoid garnet from Namibia and Madagascar rather than the horsetail inclusion scenes noted in serpentinite-related demantoid from Russia. Trace element chemistry was collected as part of an ongoing project for demantoid origin determination. Curiously, the demantoid garnets had low gallium levels ranging from 0.45 to 1.96 ppm. This is more in line with serpentine-related demantoid, with gallium less than 1 ppm, than with skarn-related demantoid, which always has gallium levels above 2 ppm. Chromium was also below detection limits, which is consistent with iron-colored demantoid from skarn-related deposits. While these Sonoran demantoid and other garnets are not currently on the market, the miners have produced up to 7 kg of the material over the last 10 years.

Aaron Palke
GIA, Carlsbad

An unusual partially non-nacreous *Pinctada radiata* natural blister pearl. The vast majority of pearls produced by the different *Pinctada* species display a lustrous nacreous surface structure. However, a small percentage of these pearls exhibit non-nacreous surfaces. GIA's Mumbai laboratory received one very interesting example for scientific examination: a partially non-nacreous natural blister pearl, obtained from the waters of Bahrain by a noted pearl diver in March 2023.

The shell weighed 21 g and measured approximately 64.55 × 63.90 × 7.72 mm. The back of the shell showed fine layered striations toward one end and areas of massive parasite holes toward the center and hinge area. The inner surface was silvery cream in color with strong orient and held a large light cream and brownish black baroque pearl, measuring approximately 11.39 × 9.31 × 8.69 mm, attached close

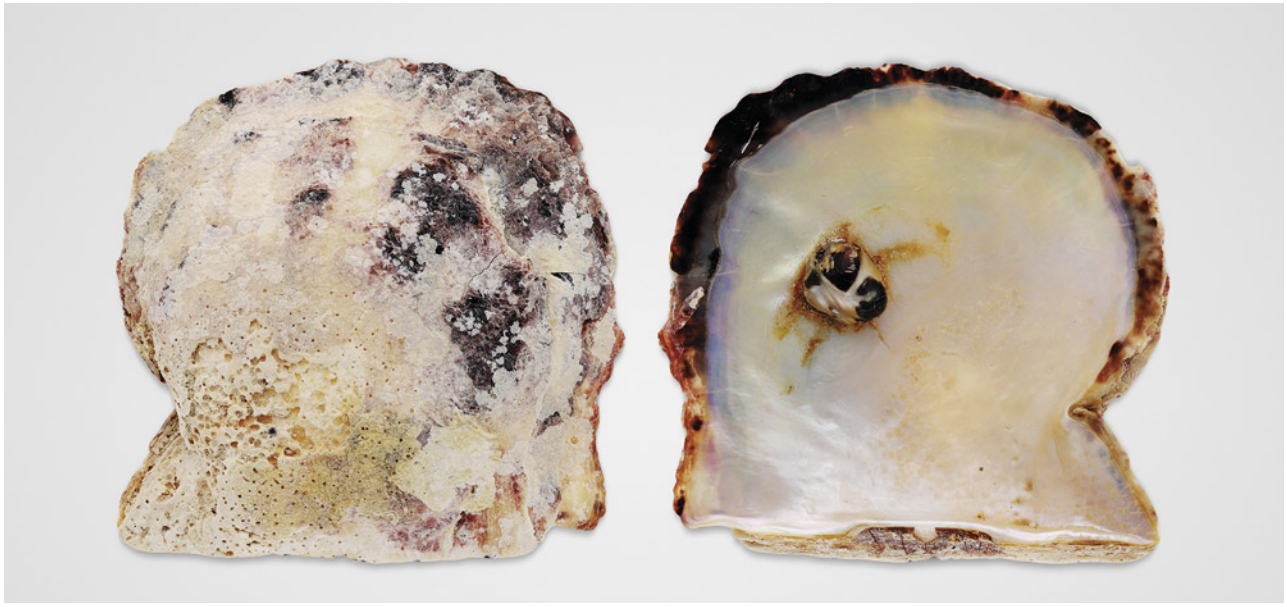

Figure 7. Pinctada radiata *shell with a natural blister pearl measuring approximately 11.39 × 9.31 × 8.69 mm. Photo by Gaurav Bera.*

to the upper mantle-lip area (figure 7). This blister pearl was very unusual compared to those typically found in the *Pinctada radiata* mollusk. Viewed under 40× magnification, the inner shell's brown edges exhibited columnar calcite honeycomb-like structures, while the white portion displayed the typical platy structure of fine nacreous overlapping aragonite platelets, presenting a chalky appearance near the hinge. Surrounding the central blister pearl was a yellowish brown region consisting of desiccated organic matter.

A closer look at the light cream, strongly iridescent section of the blister pearl with the distinctive platy structure looked more like "fingerprints," distinctly separated by a delineated step feature from the adjacent black area. The black region was noticeably dull and matte and covered by a translucent layer revealing circular botryoidal surface spirals with a calcitic columnar pattern. Additionally, significant surface-reaching cracks were present in the translucent black area along the columnar structures (figure 8, left). Within the non-nacreous "cellular" structure, a layer had peeled off, accentuating the light cream calcitic step feature (figure 8, right).

Real-time microradiography imaging of the blister pearl and its host shell revealed a distinct outline showing the point of attachment of the pearl to the shell. An organic-rich

Figure 8. Left: Partially non-nacreous blister pearl showing significant surface-reaching cracks (blue arrow) and a distinct delineated step feature separating the light cream area from the adjacent black area (red arrow). Right: A columnar honeycomb-like calcite structure was observed at the edge of the step feature; field of view 14.40 mm. Photos by Karan Rajguru.

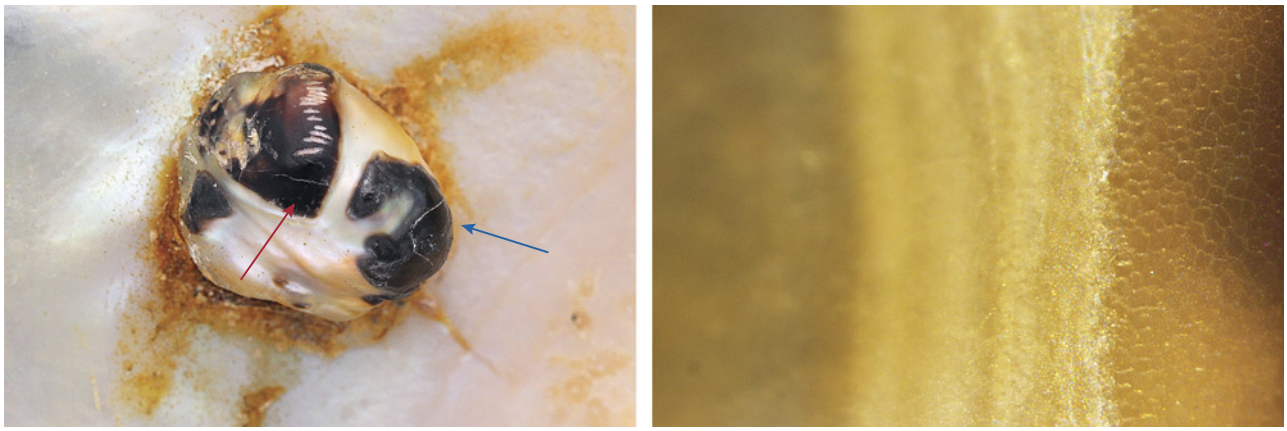

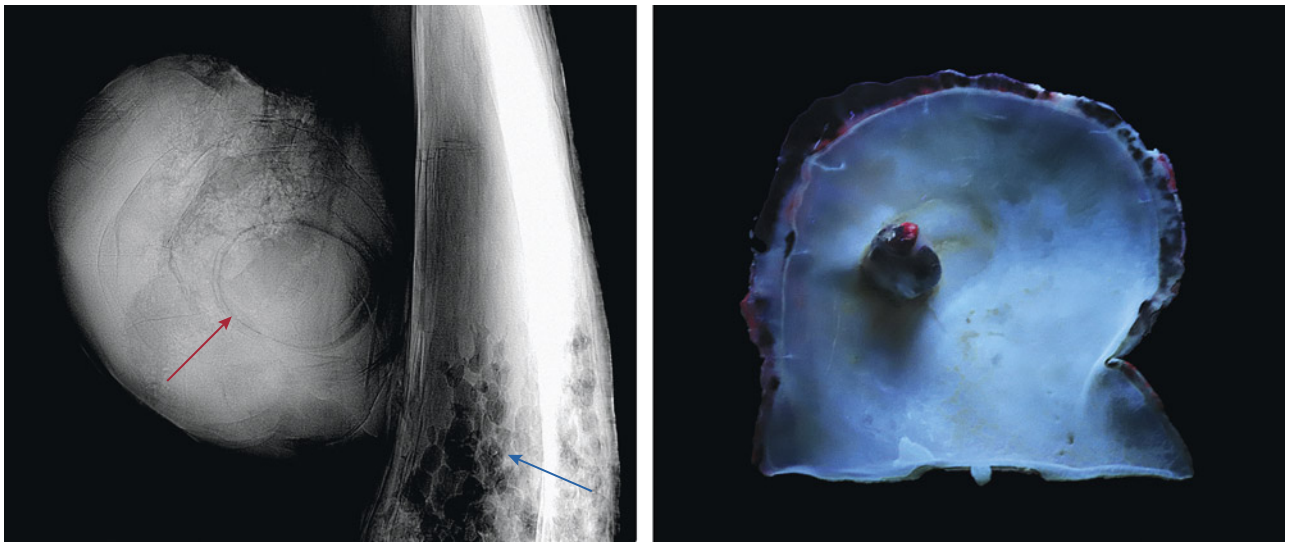

Figure 9. Left: A real-time microradiograph image showing the internal structure of the blister pearl consisting of an organic-rich core surrounded by concentric growth arcs (red arrow) with parasite holes in the host shell (blue arrow). Right: Strong orangy red reaction under long-wave UV light, observed on the edge of the shell and part of the black area on the blister pearl. Photos by Lubna Sahani (left) and Gaurav Bera (right).

core with contrasting patchy light and dark gray areas occupied almost half of the pearl's internal structure (figure 9, left). This was surrounded by concentric growth arcs, which are classic features of natural pearl structures, similar to those observed in known *Pinctada radiata* pearls from GIA's research database. In addition, significant cracks extending from the pearl to the shell and parasite tubes forming a dendritic pattern in the host shell were seen when the pearl was X-rayed in other directions. The structure indicated a natural whole pearl that had attached itself to the host shell ("Natural shell blisters and blister pearls: What's the difference?" *GIA Research News*, August 26, 2019).

Due to the limitations imposed by the size of the shell, it was not possible to collect chemical data on the pearl using energy-dispersive X-ray fluorescence spectrometry. However, both shell and pearl showed an inert reaction when exposed to X-ray fluorescence, indicative of its saltwater origin. An interesting reaction was observed under long-wave ultraviolet light. The edge of the shell and part of the black area on the pearl showed a strong orangy red fluorescence, while the inner part of the shell displayed a weak blue reaction (figure 9, right). The shell was inert under short-wave UV. Similar reactions linked to a type of porphyrin pigment have been observed in partially non-nacreous and nacreous pearls from the *Pteria* species (S. Karampelas, "Black non-nacreous natural pearls from *Pteria* species," *Journal of Gemmology*, Vol. 35, No. 7, 2017, pp. 590–592). Raman spectroscopy using 514 nm and 814 nm laser excitation revealed peaks at 701/704 cm^{-1} and 1086 cm^{-1}, indicative of aragonite. Due to high fluorescence, no calcitic peaks were observed in the non-nacreous area. Photoluminescence spectra collected from both the shell and the blister pearl revealed three broad peaks centered at 620, 650, and 680 nm, which are characteristic of some naturally colored pearls.

Formation of natural blister pearls in the wild has always been an interesting topic of research for gemological laboratories. The studied sample is certainly noteworthy due to its size, partially non-nacreous structure, and unique reaction under long-wave ultraviolet light.

Abeer Al-Alawi, Lubna Sahani, Karan Rajguru, and Roxane Bhot Jain
GIA, Mumbai

A unique omphacite jade pendant. In the past decade, omphacite jade with strong to vivid green color has increased in popularity. Especially noteworthy is the high-quality omphacite jade now coming from Guatemala. There are generally two types of omphacite jade. The first, commonly known as "black omphacite jade" (*mo cui* in Chinese), is typically opaque to semitranslucent and black to dark green. The second type contains higher chromium content and is usually made into cabochons, tablets, and pendants of 2–3 mm thickness to produce a strong green color and semitransparent appearance.

Recently, a carved pendant measuring 68.4 × 39.9 × 6.4 mm was submitted to the Taiwan Union Lab of Gem Research (TULAB) for identification (figure 10). The pendant was semitranslucent; its color appeared black when viewed under reflected light but dark green and yellow when viewed with transmitted light. Due to the pendant's uneven surface, its refractive indexes were challenging to measure. The dark

Figure 10. An omphacite jade pendant measuring 68.4 mm tall, shown in reflected light (left) and transmitted light (right). Photo by Tsung-Ying Yang.

green part showed a refractive index of approximately 1.67, and that of the yellow part was around 1.71 (both by spot reading). To further confirm the mineral composition, Raman spectroscopy with 785 nm excitation was performed on the yellow and dark green areas. The spectra were compared with the RRUFF database (Lafuente et al., 2015, https://rruff.info/about/downloads/HMC1-30.pdf) in figure 11, and the results indicated that the main component of the dark green portion of this pendant was omphacite. However, the yellow regions were identified as vesuvianite, constituting approximately 30% of the entire piece. Omphacite jade displaying both dark green omphacite and paragenetic yellow vesuvianite are not common.

From a gemological perspective, this green and yellow pendant is undoubtedly an exceptional case, given the rarity of omphacite jade coexisting with vesuvianite. However, precisely calculating the amounts of omphacite and vesuvianite with destructive X-ray diffraction analysis was not possible.

Shu-Hong Lin
Institute of Earth Sciences,
National Taiwan Ocean University
Taiwan Union Lab of Gem Research, Taipei

Tsung-Ying Yang, Kai-Yun Huang, and Yu-Shan Chou
Taiwan Union Lab of Gem Research, Taipei

Star beryl. Asterism is not a common phenomenon in beryl species, but it has previously been reported in emerald and aquamarine (K. Schmetzer et al., "Asterism in beryl, aquamarine and emerald – an update," *Journal of Gemmology*, Vol. 29, No. 2, 2004, pp. 65–71; Fall 2015 Gem News International, pp. 334–335). Recently, the author observed several star black beryl bead bracelets purchased from a Chinese e-commerce platform. For this report, four beads with noticeable asterism were collected for testing. The material was called "Devil Blue" aquamarine. The beads ranged from 9.11 to 9.47 mm in diameter and displayed a star phenomenon.

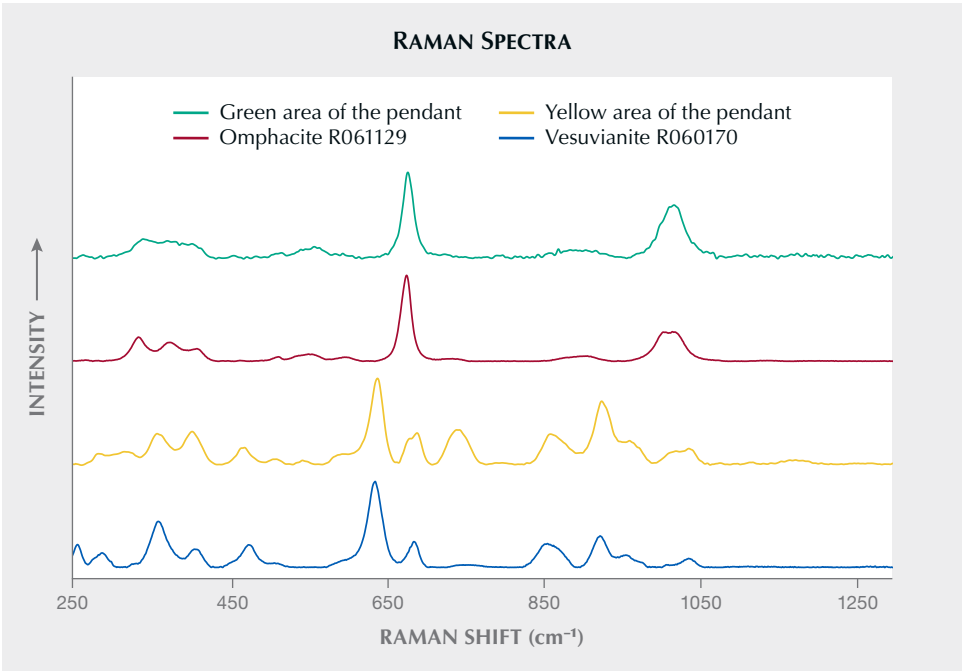

Figure 11. Comparisons between the Raman spectra of the jade pendant and the spectra of RRUFF database. The results confirmed that the green part of the jade pendant is omphacite and the yellow part is vesuvianite. The stacked spectra are baseline-corrected and normalized.

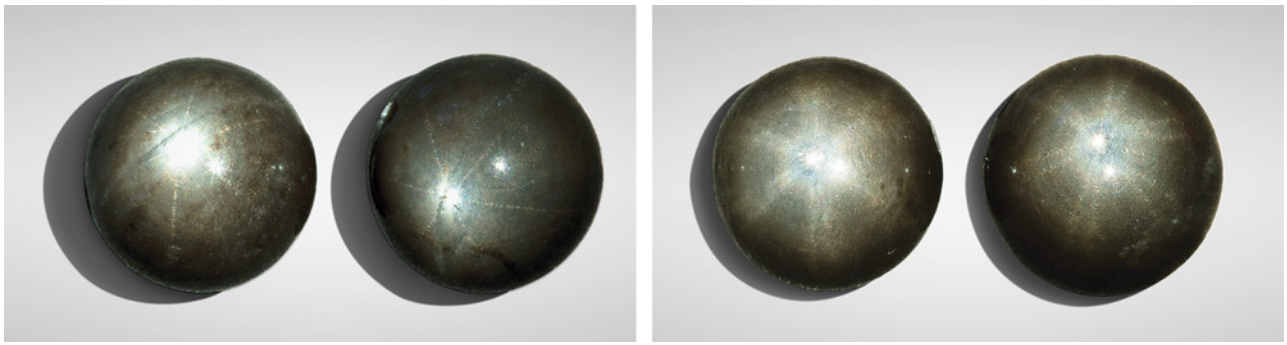

Figure 12. Left: Black beryl beads displaying six-rayed stars. Right: Black beryl beads displaying twelve-rayed stars. Photos by Tinh Xuan Nguyen.

Of the four beads, two had six-rayed stars with arms intersecting at 60° angles (figure 12, left) and two had twelve-rayed stars with two sets of six-rayed stars located in the same concentric point but with different orientations—the two stars were offset by approximately 10° (figure 12, right). Gemological testing of the beads provided the following characteristics: a hydrostatic specific gravity varying from 2.67 to 2.73, a spot refractive index of 1.57, an inert reaction under long-wave and short-wave UV, and no diagnostic absorption spectrum. These properties were consistent with beryl. Raman analysis confirmed the material was beryl.

Figure 13. The observed asterism was due to oriented iridescent needle inclusions. Several dark intersecting lines with lower relief are from the hexagonal growth structure of beryl. Photomicrograph by Tinh Xuan Nguyen; field of view 0.5 mm.

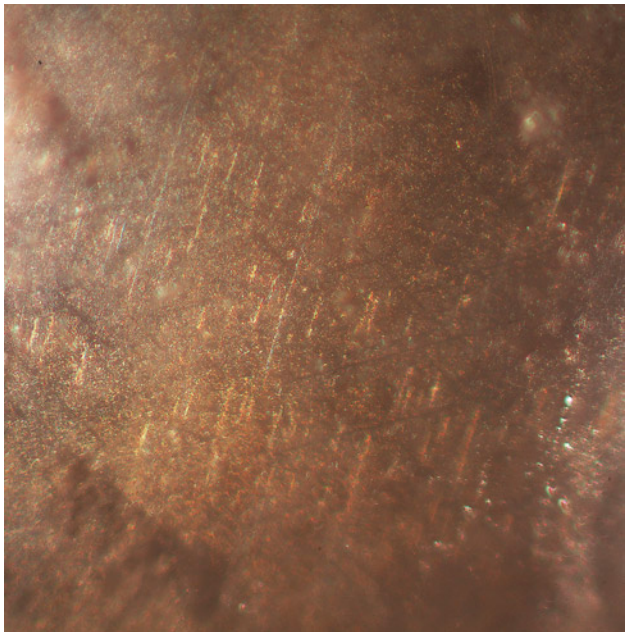

Under the microscope, we observed numerous needle inclusions oriented perpendicular to the *c*-axis and parallel to the three *a*-axes, which caused the asterism (figure 13). Moreover, the needles were concentrated as layers, forming multiple parting planes (figure 14) parallel to the basal pinacoid plane in all beads. This parting, combined with the presence of twelve-rayed stars, suggested that the growth orientation of this beryl was changing during the growth process. Additionally, the samples also showed an intersecting structure (figure 13) with angles of 120°/60° that resembled part of the hexagonal growth structure previously observed on the pinacoid of an aquamarine (Spring 2022 *G&G* Micro-World, pp. 70–71). This structure highlights that the asterism is oriented perpendicular to the *c*-axis, allowing the easy determination of this direction in translucent to opaque beryl.

Tinh Xuan Nguyen
PNJ Laboratory Company Ltd.
Ho Chi Minh City

Figure 14. Multiple parting planes, illustrated by parallel lines lying perpendicular to the c*-axis, represent the differing concentrations of oriented needle inclusions occurring during growth. Photomicrograph by Tinh Xuan Nguyen; field of view 0.5 mm.*

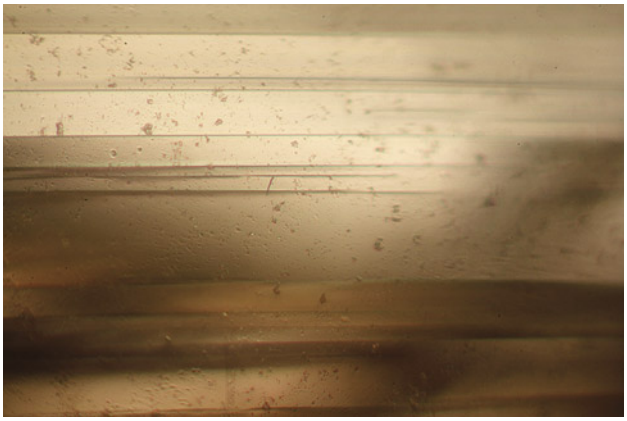

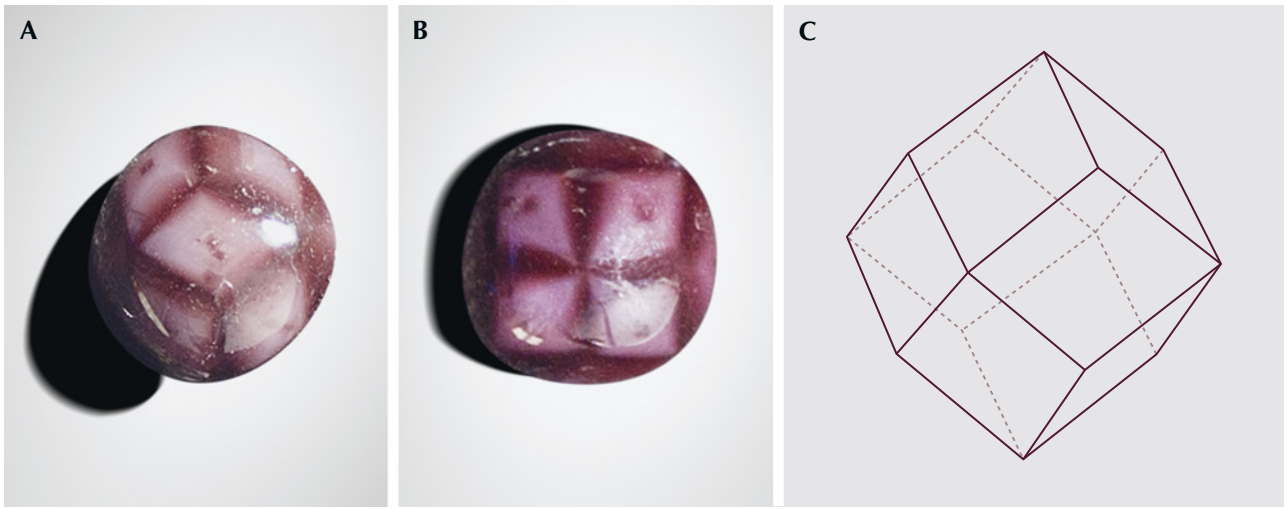

Figure 15. The color zoning in this 3.57 ct almandine garnet creates a cross structure that forms three-arm (top of A) and four-arm trapiche patterns (B) at every intersecting point of the crystal. These color zones are arranged along the edges of the dodecahedron (C). Photos by Le Ngoc Nang.

Trapiche garnet from Vietnam. The garnet group contains the most gem-quality species for jewelry manufacturing. Phenomenal garnets such as almandine and pyrope species are also known for their four- and six-rayed asterism. Nevertheless, the trapiche structure found in emerald, ruby, sapphire, tourmaline, and quartz is extremely rare in garnet. This structure can be considered an immobile star phenomenon. Inclusions and color zoning are responsible for the formation of two-, four-, or six-arm trapiche patterns.

Recently, the authors received a garnet sample originating from Thac Ba Lake in the Yen Bai province of Vietnam, obtained by a local miner. The 3.57 ct polished gem was pinkish white and reddish brown, translucent to opaque, and measured 7.11 × 6.90 × 6.40 mm. The diamond-shaped pinkish white portions were surrounded by reddish brown color zones, creating three-arm and four-arm trapiche patterns (see the video clip at www.gia.edu/gems-gemology/winter-2023-gemnews-trapiche-garnet).

Gemological testing revealed the sample's specific gravity of 4.16 and refractive index of 1.78. The stone displayed absorption spectra with distinct bands at 504, 520, and 573 nm, and it was inert under ultraviolet light for both long-wave and short-wave. All the data confirmed the almandine garnet species.

Observing all sides of the stone, we identified 14 trapiche patterns, including 6 four-arm and 8 three-arm patterns, surrounding 12 diagonal faces (figure 15). The arms grew outward from the center of the four-arm trapiches and inward for the three-arm trapiches. While the reddish brown portions extended along the edges of the garnet crystal, the diagonal lines formed the faces of the rhombic dodecahedron crystal, a typical crystal habit of almandine originating from metamorphic rock. Interestingly, when illuminated with a flashlight, the trapiche patterns glowed a fascinating vivid red and outlined the diamond-shaped portions in sharp contrast (figure 16).

Using the gemological microscope, we found that the reddish brown color zones were not colored by inclusions. In contrast, we hypothesized that the reddish hue might be induced by the dispersion of metal ions—in this case, iron (E. Fritsch and G.R. Rossman, "An update on color in gems. Part 1: Introduction and colors caused by dispersed metal ions," Fall 1987 *G&G*, pp. 126–139). The position of the color zoning along the edges of the crystal might be explained by the concentration of coloration elements in the crystal's symmetrical planes. The reddish brown zones had higher transparency than the crystal planes, producing a "glowing net" when shining a light through the stone.

Figure 16. This 3.57 ct garnet emits vivid red through the trapiche patterns when shining a flashlight through the gem. Photo by Le Ngoc Nang.

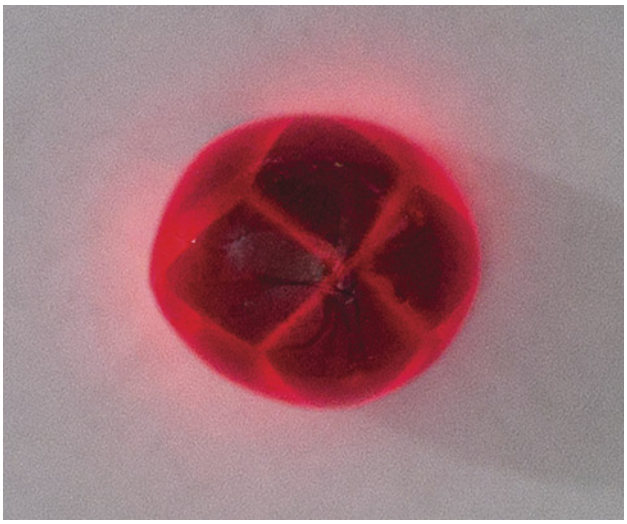

Although the trapiche pattern has been observed in several gems, it is rarely seen in garnet. The 14 trapiche patterns together in one specimen make this garnet unique.

Le Ngoc Nang, Ho Nguyen Tri Man, and Pham Minh Tien
Liu Gemological Research and Application Center
Ho Chi Minh City

Pyritized triceratops fossils from South Dakota. In recent years, the Hell Creek Formation spanning the Dakotas, Montana, and Wyoming has been extensively studied by paleontologists. This rock formation is home to fossils of various vertebrates, including dinosaurs such as *Tyrannosaurus rex* and triceratops. The author, an amateur paleontologist, recently unearthed a new dinosaur fossil site on privately owned land in Perkins County, on the northern edge of South Dakota.

Although multiple creatures are being uncovered at the site, closer examination of these fossils recovered revealed that they were from triceratops (figure 17). In addition, the fossils contained pyrite, an iron sulfide also known as "fool's gold" that forms in sedimentary rocks, giving the fossils a striking metallic appearance. This discovery of pyrite inspired the author to cut and polish the fossils into pieces for collectors to display (figure 18). Sixteen pieces have been cut so far.

Only water was used for cutting, to avoid dust inhalation and to keep the specimens from turning black. A cerium oxide polishing compound was used for the finish, followed by a drying process. The pieces were then treated with an epoxy adhesive to prevent pyrite decay.

The newfound dinosaur site in the Hell Creek Formation of South Dakota holds the promise of unveiling more treasures from the past. As the author's team and others dive deeper into the site, they hope to uncover additional fossils, providing insight into the long-lost world of dinosaurs.

Deven Fisher
Rapid City, South Dakota

Figure 17. Triceratops fossils recovered from the Hell Creek Formation in South Dakota. Photo by SD Gem & Fossil.

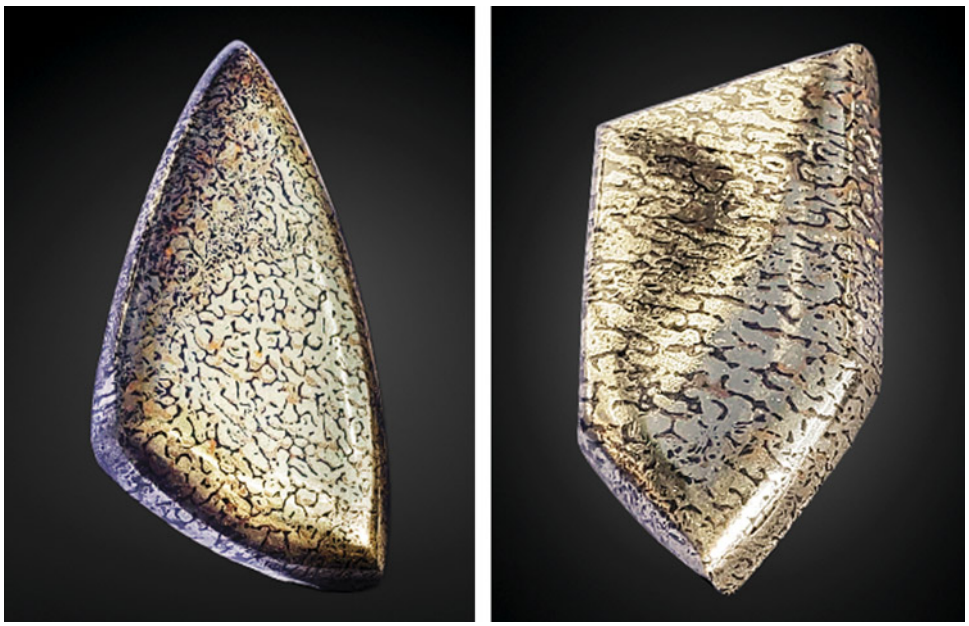

Figure 18. The cut and polished piece of pyritized triceratops fossil on the left weighs 50.5 ct and measures 41.28 × 22.23 mm. The piece on the right weighs 22.5 ct and measures 31.75 × 15.88 mm. Photos by SD Gem & Fossil.

Figure 19. The "Infinite Blue," an 11.28 ct Fancy Vivid blue diamond, sold for $25.3 million in Hong Kong. Courtesy of Sotheby's.

Figure 20. Selling for $44 million, the 17.61 ct Internally Flawless "Bleu Royal" became the most expensive auction jewel of 2023. Courtesy of Christie's Images Ltd. 2023.

AUCTION REPORT

Fall 2023 auction highlights. Following the controversial three-part sale of Heidi Horten's jewels in the spring (Summer 2023 GNI, pp. 254–256), Christie's announced the cancellation of the fourth sale ahead of the fall auction season. The late Austrian billionaire's estate made headlines earlier in the year because of her husband's connection to Nazi Germany, resulting in considerable backlash against Christie's despite their pledge to donate part of commissions to Holocaust-related charities.

In early October, Sotheby's kicked off the season with a single-lot sale of the 11.28 ct "Infinite Blue" (figure 19) in Hong Kong. Celebrating its 50th year in Asia, the auction house offered the Fancy Vivid blue type IIb diamond from the Cullinan mine in South Africa set in a ring with a pink diamond halo and colorless diamond side stones. With GIA's highest color grade for a blue diamond, the ring sold for $25.3 million, just below the low end of its presale estimate.

Another blue diamond achieved better results in early November. The pear-shaped "Bleu Royal" (figure 20), a 17.61 ct Internally Flawless Fancy Vivid blue, was offered by Christie's in Geneva as the largest diamond of its color to ever appear at auction. Set in a ring that also featured two pear-shaped colorless diamonds of approximately 3 ct each, the piece became the most expensive auction jewel of 2023. After seven minutes of bidding, the ring featuring the GIA-graded type IIb diamond sold for $44 million, near the higher end of its presale estimate.

The "Pink Supreme" (figure 21), a 15.48 ct Internally Flawless Fancy Intense pink diamond and the largest of its kind ever offered at auction, sold for $10.8 million at

Figure 21. A ring featuring the "Pink Supreme," a 15.48 ct Internally Flawless Fancy Intense pink diamond, sold in Hong Kong for almost $11 million. Courtesy of Christie's Images Ltd. 2023.

Christie's Magnificent Jewels sale in Hong Kong on November 27. Set in a gold ring with pear-shaped and round colorless diamonds, the GIA-graded type IIa gem belonging to a private collector sold within its presale estimate.

In a season filled with plot twists, some highly advertised and anticipated pieces did not go under the hammer on auction day. The "Blue Lagoon," a 93.94 ct blue Paraíba tourmaline and the top lot for Sotheby's Magnificent Jewels in Geneva, was withdrawn before the auction went live. In the final Magnificent Jewels auction of the season in New York, Christie's promoted the "California Sunset" diamond earrings as their top lot. Featuring a stunning pair of Fancy Vivid orange-yellow diamonds weighing approximately 12 ct each, the earrings, estimated to fetch up to $12 million, were also a no-show.

Erica Zaidman
GIA, Carlsbad

RESPONSIBLE PRACTICES

Artisanal diamond mining: Addressing the knowledge gap. In the developed world, the word *diamond* immediately evokes the allure and sparkle of a polished brilliant. What does the word mean, however, for an artisanal diamond miner living in poverty?

Artisanal diamond mining accounts for 20% of global production and significantly impacts millions of lives in the developing world, particularly in Africa. "Artisanal" simply implies that the tools and equipment used by the miners are rudimentary. This type of mining is conducted predominantly by individuals, small groups, or families, who frequently migrate in search of the next deposit. The work is subsistence labor, and the miners typically sell to anyone willing to buy (often without the luxury of a legal transaction). Despite its numerous challenges, which also include smuggling and human rights abuses, artisanal mining is their principal form of income. But beyond the fact that diamonds can be exchanged for subsistence money, what do these miners know about them?

In many countries where artisanal mining is prevalent, miners often have an innate and comprehensive understanding of the material. For example, Sri Lankan gem miners can expertly locate and sort through the *illam* (gem gravel) and differentiate between the fine-quality and lesser-quality material. They have been doing this for thousands of years. But diamond mining is different, particularly in Africa, where the first known primary deposit was discovered less than 200 years ago. In the twentieth century, the system of grading based on the Four *C*s (color, cut, clarity, and carat weight) established a framework for price setting in the diamond trade. This pricing system for polished material underlies the value of rough material and determines its selling price. Therefore, understanding the Four *C*s is vital to the effective trade of diamond rough.

However, the majority of artisanal miners in Africa do not yet have a strong working knowledge of rough diamond, placing them at a significant disadvantage when negotiating the price of rough with buyers. In 2022, the NGO Diamonds for Peace conducted basic training on rough diamond grading for Liberian miners (figures 22 and 23), a project funded by the World Bank and operating in collaboration with Empowerment Works Incorporated.

Liberia's first major diamond deposit was discovered in 1957 along the Lofa River, close to the border of Sierra Leone to the north, which has much higher diamond pro-

Figure 22. Artisanal mining in Liberia. Courtesy of Diamonds for Peace.

Figure 23. Miners sorting through gem gravel. Courtesy of Diamonds for Peace.

duction. Currently, figures stand at around 50,000 carats per annum. Production peaked at 600,000 carats annually in the 1970s (although most of that figure could be attributed to smuggled material coming in from bordering countries). Two civil wars, starting with a military coup in 1980, resulted in export sanctions imposed by the United Nations. Since 2007, when the country joined the Kimberley Process, diamond has been reestablished as an important mineral resource, particularly with the recent discovery of diamond-bearing kimberlites. These deposits have not been commercially exploited. Instead, the mining remains artisanal and the material is found primarily in alluvial placers along the Lofa River.

In pre-training interviews given to establish each miner's level of knowledge, numerous misconceptions became evident. For instance, they valued a diamond based on carat weight alone, regardless of quality, color, and potential yield. They had also been told that colored diamonds have no value. Such diamond "myths" have disseminated over the past fifty years, and buyers are often quick to exploit the miners' lack of knowledge.

For artisanal diamond mining to benefit the future of Liberian communities, the diamonds need to be traded for a price that reflects their real-time value according to their potential polished price (figure 24). The diamonds must be fed into the supply chain correctly, and the economic gain

Figure 24. A parcel of rough diamonds, collected over a month by a Liberian artisanal miner. The diamond indicated by the arrow weighs 0.80 ct. Photo by Beth West.

needs to find its way back into these rural communities. This boomerang-back of benefit is no easy feat in West Africa.

Yet small steps toward progress can be made by adjusting the information asymmetry. These artisanal miners need to understand the material they are working with. At the very least, it will give them a little more cash in their pocket and a slightly more comfortable standard of living. Regardless of the big picture, a simple win on that level is easily achievable.

Knowledge—and the sharing of it—is the key to building a stronger and more equitable supply chain. It is one thing for the supply chain to be traceable, but quite another for it to be equitable and ethical. To level the playing field, each player must be equally empowered. One thing that allows for such empowerment is knowledge. It is a simple right.

Diamonds for Peace, in collaboration with the author, is currently working on a next-stage "train to teach" program for the miners.

Beth West
Diamonds for Peace
London

More on Virtu Gem's ethical supply chain practices. We first covered Virtu Gem at the 2023 Ethical Gem Fair in Tucson (see Spring 2023 GNI, pp. 122–125). Virtu Gem gives artisanal and small-scale miners, traders, and cutters in Kenya, Malawi, and Zambia formal access to the international market and offers training in cutting, basic gemology, and mine safety.

The gems Virtu Gem sells (see figure 25) are cut in the source country and tracked with Provenance Proof Blockchain. One of Virtu Gem's efforts is training artisans in cutting and polishing standards to meet international market expectations. Percy Maleta, Virtu Gem's country exporter and ambassador in Malawi, said the training has attracted many cutters there and allowed them to sell gems at premium prices.

In 2022, Virtu Gem launched the National Gem Cut Course in the three countries. In online workshops led by Adriano Mol from the University of Minas Gerais State, cutters learned facet development and brainstormed to design gem cuts to represent their nations. The resulting cuts (figure 26) resembled a cheetah head for Kenya, the *mbuna* (cichlid) fish for Malawi, and the eagle for Zambia. Buyers can order gemstones from each country in its respective cut.

Virtu Gem has received two grants from the World Bank as well as assistance from other organizations. Rio Grande donated a GemLightbox, and Virtu Gem purchased more for its three country coordinators. The GemLightboxes allow traders to upload photos and videos of gems to the online sales platform rather than export stones on consignment. In addition, Gemworld donated its *World of Color* books to each country coordinator, which help traders evaluate color and cut and set prices.

The donations have also been instrumental in Virtu Gem's work with the National Gem Cutting School in Zambia, where students use the books and GemLightboxes. Virtu Gem cofounder Susan Wheeler said there are many gem cutters in Kenya, and she would like to establish a gem cutting program for women in Malawi.

Figure 25. These indicolite tourmalines (9.27 and 6.16 ct) from Zambia are among the variety of gems Virtu Gem offers. Photo by Robert Weldon.

Figure 26. Gemstone cutters in Kenya, Malawi, and Zambia developed cuts to represent their countries in Virtu Gem's National Gem Cut Course. Left to right: the Kenya Cheetah Head, Zambia Eagle, and Malawi Mbuna *Fish cuts in aquamarine, amethyst, and rhodolite garnet. Photo courtesy of Virtu Gem.*

Wheeler said gemology students should understand the ethical issues inherent in the traditional gemstone supply chain and the importance of cutting in the source country. She emphasized the importance of knowing that prices are based on not only the gemstones but also the labor of the miner and the jewelry manufacturer and other costs.

Virtu Gem's country coordinator for Kenya, Caroline Muchira (figure 27), is a gem cutter by trade. While working full-time in logistics, she was inspired to travel more than 300 km by bus every weekend from Nairobi to Voi to visit the mines and talk to traders. "I was fascinated by the gemstones and how the miners could tell the difference between green garnet, green tourmaline, and pieces of green glass," Muchira said. She planned to study gemology in retirement, but in 2009, after the company she worked for was sold, she sold all of her belongings to earn her Graduate Gemologist diploma at GIA's Thailand school. During Muchira's visits to Voi, she saw the issues the miners faced, especially women and youth. "Often they are unable to sell their stones at a fair price to middlemen, whose aim is to strike the lowest possible deal, leaving miners barely able to eke out a living," she said. Virtu Gem's system focuses on fair pricing, and Muchira now runs the organization's pricing workshops.

Muchira's ability to earn a GG is not the norm. Maleta said many in Malawi's gem trade are interested in taking

Figure 27. Virtu Gem's Kenya country coordinator, Caroline Muchira, with Nadan tsavorite mine manager Daniel Chege (left) and owner John Kimuyu (right). Photo courtesy of Virtu Gem.

Figure 28. Participants at the 37th International Gemmological Conference, held in October 2023 in Tokyo. Photo by Masayuki Itokazu.

GIA courses but can't afford it. "In a country with more than 60,000 artisanal and small-scale miners, Malawi probably only has two or three GIA graduates," he said.

The communities Virtu Gem works with produce a wide variety of gemstones, but they have yet to access some resources. While some artisanal and small-scale mining (ASM) of emeralds occurs in Zambia, Wheeler pointed out, the miners are largely unable to access the more than 400 ASM emerald concessions in Zambia, in the same area as Gemfields. Two women they work with in Zambia have a digger but can't afford the fuel to run it. "They could be producing the same quality emerald as Gemfields," Wheeler said. "They can't afford to do it on a regular basis, and loans are very expensive. We want to support the emerald mining. So we're trying to work on how to go forward with sourcing and getting more supply with emeralds."

Virtu Gem is part of the United Nations Conscious Fashion and Lifestyle Network, which highlights collaborations that further the UN's Sustainable Development Goals (SDGs). Virtu Gem's efforts are associated with six of the SDGs: ending poverty, ending hunger, gender equality, decent work, inclusive and sustainable industrialization, and reducing inequality. "We're going to continue to align everything that we do in Virtu Gem with the Sustainable Development Goals so people can see that framework and what gemstones can do to make progress," Wheeler said.

Erin Hogarth
GIA, Carlsbad

CONFERENCE REPORTS

37th International Gemmological Conference. The 37th International Gemmological Conference (IGC) was held October 23–27 in Tokyo, with more than 80 delegates, observers, and special guests from 24 countries attending (figure 28). The IGC, which started in 1951 and takes place every two years, brings together international gemologists,

Figure 29. Left: IGC participants viewed a 102-ton jadeite boulder at the Oyashirazu jade museum in Itoigawa. Right: During a field trip to Ago Bay, participants observed the implanting of a bead nucleus in a Pinctada fucata *oyster. Photos by Ahmadjan Abduriyim.*

scholars, and researchers to present their work on natural and synthetic diamonds, colored gemstones, pearls, gem treatments, geological and geographical study of gem deposits, and more. This year, IGC delegates had the opportunity to meet with researchers from various earth science disciplines as well as Japanese laboratory gemologists and gem traders at specially organized events.

The opening ceremony began with a welcome from the Japan Jewellery Association, the Japan Gem Society, the Gemmological Society of Japan, and the IGC. Six keynote presentations followed. IGC executive secretary **Dr. Jayshree Panjikar** discussed the past, present, and future of the conference, beginning with its formation, followed by advancements in gemological science and the latest developments in instrumentation. Dr. Panjikar announced the IGC's goal of recruiting more young gemologists and scientists by its 100th anniversary in 2052, bringing greater knowledge to the general public and consumers. **Professor Hisao Kanda** (National Institute for Materials Science, Japan) described the activities of Japanese researchers from 1980 to 2000, particularly in the area of diamond synthesis. **Dr. Hanco Zwaan** (Netherlands Gem Laboratory/Naturalis Biodiversity Center, Leiden) discussed the differences between natural and laboratory-grown diamond in terms of growth history and conditions and properties. **Yuichi Nakamura** (Mie Prefecture Pearl Promotion Council) reviewed the status quo of the akoya pearl industry and initiatives for sustainable pearl cultivation in Japan. **Professor Pornsawat Watanakul** (Kasetsart University) emphasized the importance of research for the gem and jewelry industry, noting examples of in-depth research and advanced technology that are yielding applicable knowledge. **Dr. Michael Krzemnicki** (Swiss Gemmological Institute SSEF) addressed the issue of classifying colored gems into their respective varieties and presented a number of case studies to illustrate the topic from a gemological laboratory perspective.

At the main conference venue, the National Museum of Nature and Science, participants attended oral and poster presentations, along with the IGC exhibition booth and a demonstration booth showcasing recent advances. Many high-quality scientific talks were presented by IGC members, and some of the presenters were elected as new delegates. Abstracts of the 48 presentations covering topics ranging from diamonds and colored stones to technology and techniques can be viewed on the conference website at www.igc-gemmology.org/s/IGC2023_webfinal.pdf.

In addition to the academic program, the IGC Japan committee organized pre-conference and post-conference excursions (figure 29). Before the conference, 32 participants visited the jadeite gorge in the Itoigawa region of Niigata Prefecture and learned about its geological setting and formation and observed the jadeite deposit's location in serpentinite lenses within a high-pressure metamorphosed complex. After the conference, 25 participants visited the akoya cultured pearl farm at Ago Bay, where they witnessed the bead implantation process and pearl harvesting. In addition to these conference excursions, a tour of Mount Fuji and a visit to the jewelry city of Kofu were organized.

Ahmadjan Abduriyim
Tokyo Gem Science and GSTV Gemological Laboratory

ANNOUNCEMENTS

***G&G* contributors awarded for best geoscience research.** Several *G&G* authors and editorial board members are among those honored for their contributions to a recent volume in the *Reviews in Mineralogy and Geochemistry* series (figure 30). The Geoscience Information Society's annual Mary B. Ansari Best Geoscience Research Resource Award recognizes the year's outstanding reference publication or website. The 88th volume in the *Reviews* series, *Diamond: Genesis, Mineralogy and Geochemistry* is a comprehensive resource covering a wide range of diamond-related subjects. The publication is available for download at geoscienceworld.org and minsocam.org.

Congratulations to volume editors Karen Smit, Steve Shirey, Graham Pearson, Thomas Stachel, Fabrizio Nestola, and Thomas Moses, as well as *G&G* contributors Christopher M. Breeding, Jim Butler, Alan Collins, Ulrika D'Haenens-Johansson, Dorrit Jacob, Mandy Krebs, and Evan Smith for their chapters in the volume.

GIA Alumni Collective. The GIA Alumni Collective offers an exciting networking platform for GIA graduates. The online community at collective.gia.edu allows a diverse group of users to access both live and self-paced Continuing Education seminars, join virtual chapters, connect with global alumni, and more. The site also puts GIA alums in the spotlight (figure 31), celebrating those who uphold the highest standards of GIA's consumer protection mission.

Winning a 40-pound tub of historical jewelry at auction led sisters Laura Mae and Amanda Jean (last names withheld) to launch their online jewelry resale business, Maejean Vintage, in 2010. New to the industry, they both pursued Graduate Gemologist diplomas at GIA. Today they use their expertise to salvage rare and valuable historical pieces and sell them all over the world.

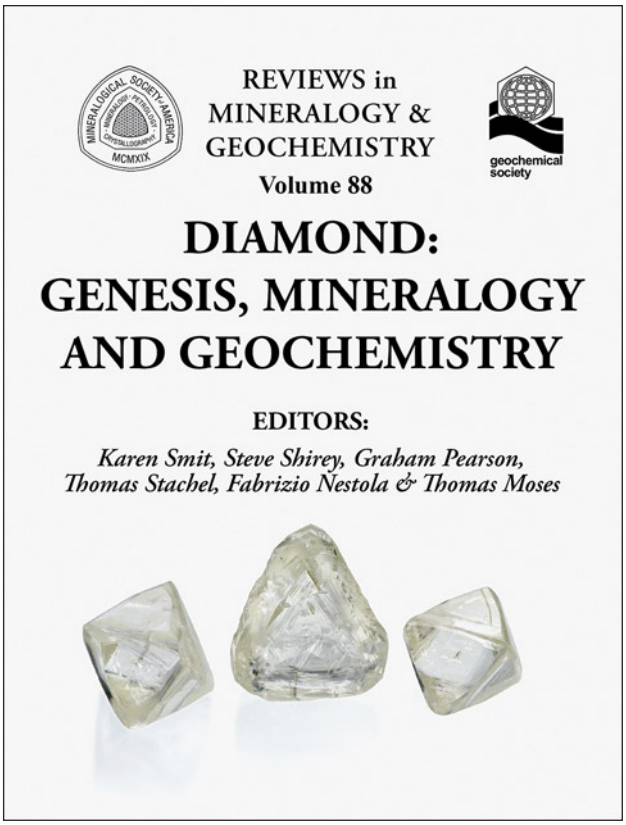

Figure 30. Diamond: Genesis, Mineralogy and Geochemistry, *Volume 88 in the* Reviews in Mineralogy and Geochemistry *series, received this year's Mary B. Ansari Best Geoscience Research Resource Award.*

Ilan Portugali's journey took him from Israel to Madagascar to Mozambique and finally to the U.S., where he worked for a diamond dealer and completed his Graduate

Figure 31. Laura Mae, Amanda Jean, and Ilan Portugali are some of GIA's featured graduates on the Alumni Collective website.

Figure 32. Heitor Barbosa discovered Paraíba tourmaline in 1989 after almost a decade of mining. Photo by Duncan Pay.

Diamonds diploma at GIA. After positions with Van Cleef & Arpels and Harry Winston, Portugali started his own business, Beverly Hills Diamonds, which sources conflict-free and fair-trade diamonds.

Visit https://collective.gia.edu/meet-the-collective.html to read stories from these alumni and more.

IN MEMORIAM

Heitor Barbosa. The discoverer of Paraíba tourmaline, Heitor Barbosa (figure 32), died September 23, 2023, at the age of 90. Driven by intuition, Barbosa began his quest in the early 1980s at an old pegmatite mine in the Brazilian state of Paraíba. After several unsuccessful years and considerable skepticism from others, Barbosa prevailed and unearthed one of the world's rarest gems—cuprian elbaite tourmaline—in 1989. Over the next two years, using simple hand tools and candles for lighting, Barbosa and his team recovered between 10 and 15 kg of the tourmaline characterized by its vivid blue and blue-green hues. Production slowed significantly in the years that followed, but Barbosa continued to work the mine, remaining hopeful that more tourmaline would be uncovered. Today, Barbosa's son Sergio maintains the mine.

Barbosa is survived by his wife, four children, and two grandchildren. We extend our condolences to his family and friends.